

Polymer Mortar Assisted Self-Assembly of Nanocrystalline Polydiacetylene Bricks Showing Reversible Thermochromism

Yu Gu,[†] Weiqiang Cao,[‡] Lei Zhu,^{*,‡} Daoyong Chen,^{*,†} and Ming Jiang[†]

Department of Macromolecular Science and The Key Laboratory of Molecular Engineering of Polymers, Fudan University, Shanghai 200433, China, and Polymer Program, Department of Chemical, Materials and Biomolecular Engineering and Institute of Materials Science, University of Connecticut, Storrs, Connecticut 06269

Received January 4, 2008

Revised Manuscript Received February 28, 2008

When properly packed in the solid state, diacetylene monomers can be topochemically polymerized into polydiacetylene by UV, γ , or strong X-ray irradiation.¹ Usually, colorless diacetylene crystals turn into blue polydiacetylene crystals, which often undergo an irreversible “blue-to-red” colorimetric transition when environmental stimuli are applied. Although this unique transition has found many applications as colorimetric sensors, its irreversibility has prevented polydiacetylenes from being repeatedly used. To achieve reversible colorimetric transition, chemical modifications of diacetylene monomers have been pursued. For example, multiple hydrogen-bonding, strong aromatic, or ionic interactions were introduced into diacetylenes by chemical modifications to enhance the bonding among the head groups in side chains. Meanwhile, these diacetylene monomer had to be assembled into well-defined physical forms, including vesicles,^{2–5} nanotubes,⁶ and Langmuir–Blodgett^{3,7–9} or solid thin films,^{4,10,11} to achieve the reversibility. Recently, inorganic nanomaterials were used as nanoscale substrates to achieve reversible thermochromism for otherwise irreversible polydiacetylenes. For example, in organic/inorganic hybrids based on mesoporous silica^{12–14} and layered double hydroxide,¹⁵ the head groups in polydiacetylene side chains were bound, either covalently or noncovalently, to the inorganic matrices, and reversible thermochromism was realized.

Despite the above successful examples, the fundamental physics of reversible colorimetric transitions and their achievability for polydiacetylenes have not yet been well-understood and still desire further study. Once the physics of reversibility is understood, we will be able to design better polydiacetylenes as versatile sensor materials. For example, using polymer blends to achieve colorimetric reversibility for polydiacetylenes appears attractive because of the flexibility and easy processability of polymeric materials. However, no reversible thermochromism has been realized for irreversible polydiacetylenes in polymer blends so far.^{16,17,34} In this work, we successfully achieved reversible thermochromism in a self-assembled poly(vinylpyrrolidone) (PVP)/poly(10,12-pentacosadiynoic acid) (PDA, an irreversible polydiacetylene in the pure form^{3,15,18}) blend via hydrogen bonding in aqueous suspensions and solid films. In particular, hierarchical self-assemblies were observed, and the “bricks and mortar” morphology¹⁹ (crystallized DA bilayers being the bricks and PVP being the mortar) was found to be

responsible for the reversible thermochromism, as shown in Scheme 1. From this study, we conclude that the physical constraint exerted on every PDA bilayers by the PVP mortar substantially assisted reversible conformational transitions in the PDA main chain, which was believed to be an important reason for the reversible thermochromism.

A method for preparing noncovalently connected micelles (NCCM) was used to fabricate PVP/DA (the monomer of PDA) nanosuspension in aqueous solution.^{20–22} Both DA and PVP are commercially available. Typically, DA was dissolved in ethanol at 1.25 mg/mL and PVP in water at 5.0 mg/mL. 0.8 mL of DA ethanol solution was added at a rate of 0.05 mL/min into 10 mL of PVP aqueous solution. Shortly, DA aggregated because of its poor solubility in the aqueous solution. Note that macroscopic DA precipitates were effectively prevented by the PVP chains gathering around the DA aggregates via hydrogen bonding between carboxyl groups in DA and carbonyl groups in PVP. (The hydrogen bonding between carboxyl groups and carbonyl groups of PVP in water or other solvents has been widely reported.^{21,23,24}) As a result, a PVP/DA nanoaggregate suspension was formed (see S1 and S2 in Supporting Information). In a control experiment, reversible thermochromism could not be achieved, when PVP and PDA were mixed using a common solvent such as ethanol.

When exposed to 254 nm UV light, the as-prepared suspension did not change its color, indicating lack of proper packing of DA molecules in the nanoaggregates. The above suspension was then dried in a beaker at 30, 50, 65, and 85 °C to obtain colorless PVP/DA films (see S1 in Supporting Information). For simplicity, the films obtained by drying at 30, 50, 65, and 85 °C are denoted as films A–D.

Films A, B, and C could be topochemically polymerized after exposure to 254 nm UV irradiation at room temperature (RT) for 30 min, and polymerized films displayed a blue color, whereas film D did not polymerize at all. DSC results (see S3 in Supporting Information) showed melting points of films A and B at 52 and 54 °C, respectively, lower than that of pure DA crystals ($T_{m,0} = 62–63$ °C). However, film C presented a melting peak at ca. 75 °C, remarkably higher than $T_{m,0}$. Film D had the lowest melting point at 47 °C, suggesting a poor crystalline packing inappropriate for topochemical polymerization.

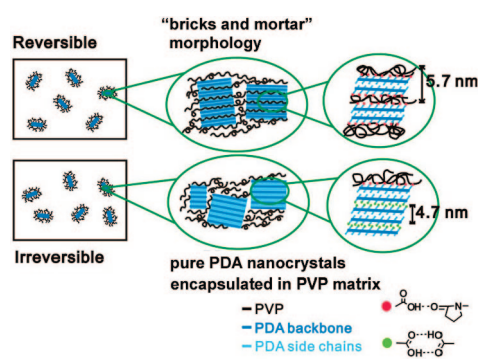
Among all polymerized films, only the polymerized film C showed reversible thermochromism between 25 and 120 °C (Figure 1-A1). Polymerized films A and B underwent an irreversible blue-to-red transition upon heating. Reversible thermochromism of polymerized film C was clearly demonstrated by UV–vis measurements between 25 and 85 °C (the highest temperature allowed by the instrument) in Figure 1-A2. At 25 °C, the film had a maximum absorption at 638 nm, responsible for the blue color. Upon heating, the maximum absorption continuously shifted to lower wavelengths, and the absorption intensity at 638 nm gradually decreased. At 85 °C, the 638 nm absorption completely disappeared, and the absorption at 586 nm increased to a maximum, with a shoulder at 540 nm. Upon cooling, the absorption spectrum changed inversely. The complete thermochromic reversibility between 25 and 85 °C was demonstrated by the fact that the spectrum at 25 °C after the heating–cooling cycle almost overlapped with that before the thermal cycle (Figure 1-A2) and also confirmed by the parameter of “colorimetric response” (CR) in different

* Corresponding authors. E-mail: lei.zhu@uconn.edu (L.Z.); chendy@fudan.edu.cn (D.C.).

[†] Fudan University.

[‡] University of Connecticut.

Scheme 1. Schematic Illustration of the “Bricks and Mortar” Morphology and Pure PDA Nanocrystals Encapsulated in PVP Matrix Showing the Reversible and Irreversible Thermochemistry, Respectively



thermal cycles^{25,26} (Figure 1-A3 and S4 in Supporting Information).

The polymerized film C could be easily dissolved in water at room temperature (RT), leading to a transparent solution with a blue color. Dynamic light scattering (DLS) result showed existence of nanoaggregates with a $\langle D_h \rangle$ (average hydrodynamic diameter) of 452 nm (see S5 in Supporting Information). Different from the precursor PVP/DA nanoaggregates (see S2 in Supporting Information), the PVP/PDA nanoaggregates were very stable in water because no changes in the size and size distribution were detected after months. These nanoaggregates in water also underwent complete reversible thermochemistry, as demonstrated in parts B1–B3 of Figure 1. Obviously, in the polymerized film C, the nanoaggregates were individually dispersed in the PVP matrix.

Parts A–C of Figure 2 are bright-field TEM images of the nanoaggregates obtained by dissolving the polymerized film C in water, showing short nano-rod-like morphology. According to the mechanism for forming NCCM,²⁰ during DA aggregation in the aqueous solution, PVP chains should surround the nanoaggregates via hydrogen bonding so that macroscopic aggregation could be avoided. Therefore, a core–shell structure with PVP as the shell and PDA in the core should be observed. To reveal this core–shell structure, we separated the PVP/PDA nanoaggregates from excessive free PVP by centrifugal ultrafiltration, followed by staining with RuO_4 for 15 min.²¹ After staining, the core–shell structure can be clearly seen in TEM images in Figure 2B. Figure 2D shows a nanoprobe electron diffraction (ED) pattern of an individual PVP/PDA nanoaggregate (Figure 2C), revealing that these nanoaggregates contain multiple layers of single crystals. It is likely that anisotropic crystal growth of DA molecules led to the short-rod-like morphology.^{27,28}

Dissolving the irreversible polymerized films A or B in water also led to nanoaggregates with a rodlike shape (see S6 in Supporting Information). The resultant aqueous solutions showed irreversible thermochemistry as well.

To understand the difference between the reversible sample (polymerized film C) and the irreversible sample (polymerized film B), the structures of the nanoaggregates were characterized using XRD. Parts A and B of Figure 3 show small-angle X-ray scattering (SAXS) and wide-angle X-ray diffraction (WAXD) results for the reversible and irreversible samples at RT, 85 °C, and after cooling back to RT for 0 and 12 h, respectively.

The SAXS profile for the irreversible sample at RT (Irrev-RT, Figure 3A) showed a single reflection peak b at a d -spacing of 4.7 nm. We assign it to the pure PDA nanocrystals en-

capsulated in the PVP matrix (Scheme 1) because this d -spacing is consistent with the lamellar thickness of a pure PDA bilayer crystal.^{29,30} The WAXD profile (Irrev-RT, Figure 3B) shows sharp Bragg reflections from monoclinic PDA crystals. These results, together with a lower melting point of 54 °C for unpolymerized film B than $T_{m,0}$, suggested that pure DA nanocrystals were encapsulated in film B.^{31,32} After polymerization, DA nanocrystals changed into PDA nanocrystals. The irreversibility of the polymerized film B therefore is consistent with the facts that pure PDA crystals in powders or other forms do not show reversible thermochemistry.^{3,15,18} After heating to 85 °C, peak b disappeared and was replaced by a broad correlation-hole scattering peak at $q = 1.1 \text{ nm}^{-1}$ (d -spacing = 5.7 nm, Irrev-85 °C, Figure 3A), suggesting the melting of pure PDA nanocrystals. This is further confirmed by the WAXD profile at 85 °C for the irreversible sample B (Irrev-85 °C, Figure 3B), showing two amorphous halos. Note that the halo at 7.7 nm^{-1} in Figure 3B is attributed to the average distance among pyrrolidone rings in PVP. After cooling immediately back to RT (0 h), little PDA crystallinity was observed [Irrev-RT (0 h) in Figure 3B]. However, after annealing at RT for 12 h, PDA recrystallized, as demonstrated by reappearance of both SAXS and WAXD peaks [Irrev-RT (after 12 h) in Figure 3A,B].

Surprisingly, the SAXS profile for the reversible sample (polymerized film C) at RT showed two reflection peaks, i.e., peaks a and b, corresponding to 5.7 and 4.7 nm, respectively (Rev-RT, Figure 3A). Judging from the d -spacing value, peak b is the same as that for the irreversible sample (polymerized film B). The corresponding WAXD profile showed the same monoclinic PDA reflections. After heating to 85 °C, peak a persisted, whereas peak b disappeared (Rev-85 °C, Figure 3A). Meanwhile, reflection peaks due to PDA crystallinity disappeared in the WAXD profile at 85 °C (Rev-85 °C, Figure 3B). The d -spacing of 5.7 nm is larger than that of pure PDA crystals (4.7 nm). Judging from the fact that this lamellar structure even persisted at 85 °C (above the melting temperature of PDA crystals at 56 °C; see DSC results in S2 of the Supporting Information), we attribute this increase in lamellar thickness to the intercalation of PVP chains into PDA crystalline bilayers (Scheme 1). This morphology can be called as “bricks and mortar” (PDA bilayers as the bricks and PVP as the mortar). In this “bricks and mortar” structure, the carboxylic acid head groups in the side chains of each PDA bilayer were hydrogen-bonded to PVP chains. This “bricks and mortar” structure can be observed by TEM for microtomed film C (Figure 2E). In the TEM image, we can clearly see the lamellar structure; i.e., the PVP layers with a low contrast are sandwiched between neighboring PDA layers with a relatively high contrast. The average period of the lamellar structure in the TEM image is about $\sim 8 \text{ nm}$, being considerably larger than the d -spacing (5.7 nm) measured by SAXS. This implicates that the sample for microtoming was not cut along the direction perpendicular to the layers. Also from this TEM image, the sandwiched PVP layers are relatively thin (ca. 1–2 nm), as compared to the PDA layers. Again, after immediately cooling back to RT (0 h), little crystallinity was seen in Rev-RT (0 h) of Figure 3B. However, after annealing at RT for 12 h, peak b reappeared in the SAXS profile [Rev-RT (after 12 h) in Figure 3A], and crystalline reflections showed up again in the WAXD profile [Rev-RT (after 12 h) in Figure 3B].

Inferring from the mechanism of topochemical polymerization, the “bricks and mortar” structure in PVP/PDA nanoaggregates must originate from the intercalated structure in PVP/

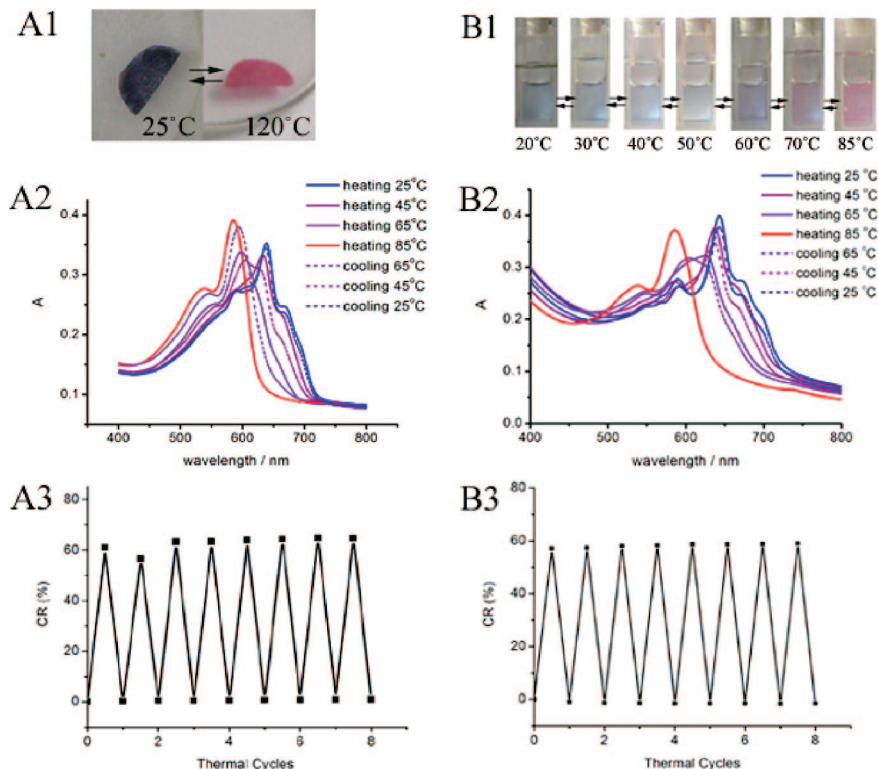


Figure 1. Photographs revealing reversible thermochromism for the polymerized film C between 25 and 120 °C (A1) and its aqueous suspension of PVP/PDA nanoaggregates between 20 and 85 °C (B1). UV-vis spectra of the polymerized film C (A2) and its aqueous suspension (B2) during heating (solid lines) and cooling (dashed lines) cycles. Colorimetric response (CR) values of the polymerized film C (A3) and its aqueous suspension (B3) during heating and cooling cycles.

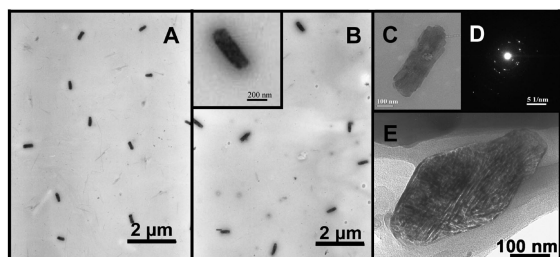


Figure 2. Bright-field TEM images (A–C) and ED pattern (D) of the PVP/PDA nanoaggregates obtained by dissolving the polymerized film (C) in water. The sample in (B) was stained by RuO₄ for 15 min. (E) shows a TEM image of the microtomed film C without staining.

DA complexes. Similar intercalated structures have been reported for hydrogen-bonding assisted polymer/surfactant

complexes by Ikkala et al.³³ Experimentally, the formation of such intercalated PVP/DA structure resulted from annealing at 65 °C, a temperature slightly higher than the $T_{m,0}$. We speculate that at 65 °C DA nanocrystals within the core of nanoaggregates melted, and either PVP chains could diffuse into DA core or DA molecules could diffuse out to the surrounding PVP chains, forming intercalated PVP/DA complex via hydrogen bonding. The complexation of DA with PVP stabilized DA lamellar crystals in the intercalated structure, and thus the intercalated structure melted at 75 °C (see S3 in Supporting Information), a temperature much higher than the $T_{m,0}$. This remarkable increase in the melting point can be attributed to a reduced entropy change during melting (or disordering) process when DA molecules were tethered to PVP layers. In comparison, when the sample was dried at lower temperatures (e.g., 30 and 50 °C

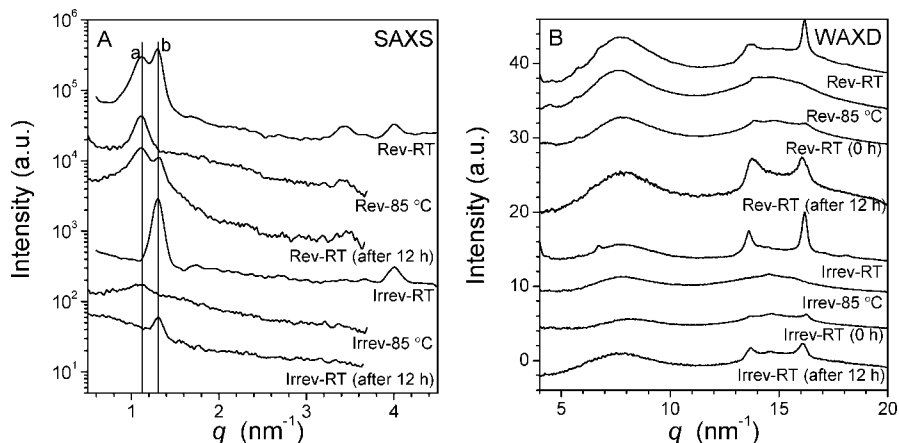


Figure 3. (A) SAXS and (B) WAXD profiles of the reversible sample (polymerized film C) and irreversible sample (polymerized film B) at RT, 85 °C, and after cooling back to RT for 0 and 12 h, respectively.

for films A and B, respectively), DA nanocrystals never melted, and thus the intercalation of PVP between DA lamellar crystals could not happen. When the film D was annealed at 85 °C, higher than the melting points of DA crystals in both the pure state (63 °C) and the intercalated structure (75 °C), the “bricks and mortar” structure was destroyed, as evidenced by the facts that film D had the lowest melting point at 47 °C and could not even be topochemically polymerized.

After topochemical polymerization of DA molecules in the intercalated crystals in film C, DA transformed to PDA and the self-assembled structure was further stabilized, because the “bricks and mortar” morphology persisted above the melting temperature of PDA crystals at 56 °C (see DSC results in S7 of the Supporting Information) until at least 120 °C.

It is widely accepted that the colorimetric transition results from changes in the effective conjugation length of polydiacetylene backbones in response to different external stimuli. If the backbones can restore to their original conformation (represented by a blue color) upon cooling back to RT, the samples are thus reversible. In principle, the conformational changes in the backbones are also substantially affected by conformational and/or positional changes in the side chains. In the present study, the red-to-blue colorimetric transition was fairly fast (in seconds) and independent of the crystallization of the side chains and/or backbones (see WAXD results in Figure 3B). We believe that a tension should exist among the side chains, when their conformation was adapted to the conformation of the backbones in red-color form. Such a tension could not be relaxed by the relocation of the side chains because their head groups were tethered to PVP layers. It might be the tendency to relax this tension that helped the backbones to restore to their original conformation in the blue-color form upon cooling.

From the SAXS results, the reversible sample (polymerized film C) appeared to contain both reversible/intercalated nanoaggregates (peak a) and irreversible/pure PDA nanocrystals (peak b) in the PVP matrix. Although the intensity of peak b in the Rev-RT curve in Figure 3A was comparable to that of peak a, we cannot obtain relative amount of reversible and irreversible samples using SAXS reflection intensities because the electron density contrasts are different for the PVP/PDA intercalated structure and pure PDA nanocrystals. However, UV-vis results in parts A2 and B2 of Figure 1 showed that the spectra at 25 °C after a heating-cooling cycle almost overlapped with those before any thermal cycle. This may suggest that the thermochromic reversibility before and after thermal cycles is nearly complete, and the fraction of irreversible PDA nanocrystals should be small. We are currently carrying out experiments to achieve 100% reversible PVP-intercalated PDA nanoaggregates.

In summary, reversible thermochromism was achieved in hierarchically self-assembled PVP/PDA nanoaggregates using a hydrogen-bonding-assisted NCCM approach. Intriguingly, a “bricks and mortar” structure in PVP/DA nanoaggregates was obtained by annealing the sample at a temperature (65 °C) slightly higher than the melting point of pure DA crystals (63 °C). After topochemical polymerization, the resultant PVP/PDA “bricks and mortar” structure was further stabilized at high temperatures (up to 120 °C). Contrary to pure irreversible PDA crystals, PVP-intercalated PDA nanoaggregates showed reversible thermochromic transitions in both aqueous suspension and dry films. The cooperative interaction between PVP and PDA through tethering carboxylic acid head groups in the side chains of PDA to PVP layers via hydrogen bonding is believed to be responsible for reversible conformational transitions between

the “red” and “blue” states. This study not only opens a new avenue for further understanding of reversible thermochromism in polydiacetylenes but also leads to more effective ways of preparing thermally reversible polydiacetylene-based materials utilizing commercially available polymers and diacetylene monomers.

Acknowledgment. The National Science Foundation of China (NSFC) (20574014, 50773011, and 20528405) is acknowledged for supporting this work. The synchrotron X-ray experiments were carried out at the NSLS of BNL, supported by the U.S. Department of Energy. Assistance from Yimin Mao, Feng Zuo, and Prof. Benjamin Hsiao at Stony Brook University for synchrotron X-ray experiments is highly acknowledged.

Supporting Information Available: Experimental section; determination of most stable PVP/DA nanoaggregate aqueous suspension; DSC curves of PVP/DA films dried at different temperatures; colorimetric response study; dynamic light scattering of reversible PVP/PDA nanoaggregates in aqueous suspension and explanation to the difference between the size of PVP/PDA nanoaggregates and that of precursor PVP/DA nanoaggregates; bright-field TEM image for irreversible sample B; DSC curves of reversible and irreversible PVP/PDA films with various thermal histories. This material is available free of charge via the Internet at <http://pubs.acs.org>.

References and Notes

- (1) Carpick, R. W.; Sasaki, D. Y.; Marcus, M. S.; Eriksson, M. A.; Burns, A. R. *J. Phys.: Condens. Matter* **2004**, *16*, R679.
- (2) Lee, S.; Kim, J. M. *Macromolecules* **2007**, *40*, 9201.
- (3) Kim, J. M.; Lee, J. S.; Choi, H.; Sohn, D.; Ahn, D. J. *Macromolecules* **2005**, *38*, 9366.
- (4) Jonas, U.; Shah, K.; Norvez, S.; Charych, D. H. *J. Am. Chem. Soc.* **1999**, *121*, 4580.
- (5) Singh, A.; Thompson, R. B.; Schnur, J. M. *J. Am. Chem. Soc.* **1986**, *108*, 2785.
- (6) Lee, S. B.; Koepsel, R. R.; Russell, A. J. *Nano Lett.* **2005**, *5*, 2202.
- (7) Ahn, D. J.; Chae, E. H.; Lee, G. S.; Shim, H. Y.; Chang, T. E.; Ahn, K. D.; Kim, J. M. *J. Am. Chem. Soc.* **2003**, *125*, 8976.
- (8) Deckert, A. A.; Fallon, L.; Kiernan, L.; Cashin, C.; Perrone, A.; Encalade, T. *Langmuir* **1994**, *10*, 1948.
- (9) Mino, N.; Tamura, H.; Ogawa, K. *Langmuir* **1991**, *7*, 2336.
- (10) Yuan, Z. Z.; Lee, C. W.; Lee, S. H. *Angew. Chem., Int. Ed.* **2004**, *43*, 4197.
- (11) Pang, J. B.; Yang, L.; McCaughey, B. F.; Peng, H. S.; Ashbaugh, H. S.; Brinker, C. J.; Lu, Y. F. *J. Phys. Chem. B* **2006**, *110*, 7221.
- (12) Peng, H. S.; Tang, J.; Yang, L.; Pang, J. B.; Ashbaugh, H. S.; Brinker, C. J.; Yang, Z. Z.; Lu, Y. F. *J. Am. Chem. Soc.* **2006**, *128*, 5304.
- (13) Peng, H. S.; Tang, J.; Pang, J. B.; Chen, D. Y.; Yang, L.; Ashbaugh, H. S.; Brinker, C. J.; Yang, Z. Z.; Lu, Y. F. *J. Am. Chem. Soc.* **2005**, *127*, 12782.
- (14) Yang, Y.; Lu, Y. F.; Lu, M. C.; Huang, J. M.; Haddad, R.; Xomeritakis, G.; Liu, N. G.; Malanoski, A. P.; Sturmayer, D.; Fan, H. Y.; Sasaki, D. Y.; Assink, R. A.; Shelnutt, J. A.; van Swol, F.; Lopez, G. P.; Burns, A. R.; Brinker, C. J. *J. Am. Chem. Soc.* **2003**, *125*, 1269.
- (15) Itoh, T.; Shichi, T.; Yui, T.; Takahashi, H.; Inui, Y.; Takagi, K. *J. Phys. Chem. B* **2005**, *109*, 3199.
- (16) Chae, S. K.; Park, H.; Yoon, J.; Lee, C. H.; Ahn, D. J.; Kim, J. M. *Adv. Mater.* **2007**, *19*, 521.
- (17) Kim, J. M.; Lee, Y. B.; Chae, S. K.; Ahn, D. J. *Adv. Funct. Mater.* **2006**, *16*, 2103.
- (18) Kim, J. M.; Chae, S. K.; Lee, Y. B.; Lee, J. S.; Lee, G. S.; Kim, T. Y.; Ahn, D. J. *Chem. Lett.* **2006**, *35*, 560.
- (19) Boal, A. K.; Ilhan, F.; DeRouchey, J. E.; Thurn-Albrecht, T.; Russell, T. P.; Rotello, V. M. *Nature (London)* **2000**, *404*, 746.
- (20) Chen, D. Y.; Jiang, M. *Acc. Chem. Res.* **2005**, *38*, 494.
- (21) Yuan, X. F.; Jiang, M.; Zhao, H. Y.; Wang, M.; Zhao, Y.; Wu, C. *Langmuir* **2001**, *17*, 6122.
- (22) Zhang, Y. W.; Jiang, M.; Zhao, J. X.; Zhou, J.; Chen, D. Y. *Macromolecules* **2004**, *37*, 1537.
- (23) Sukhishvili, S. A.; Granick, S. *Macromolecules* **2002**, *35*, 301.
- (24) Iliopoulos, I.; Audebert, R. *Macromolecules* **1991**, *24*, 2566.
- (25) Rangin, M.; Basu, A. J. *Am. Chem. Soc.* **2004**, *126*, 5038.
- (26) Okada, S.; Peng, S.; Spevak, W.; Charych, D. *Acc. Chem. Res.* **1998**, *31*, 229.

- (27) Gohy, J. F.; Lohmeijer, B. G. G.; Alexeev, A.; Wang, X. S.; Manners, I.; Winnik, M. A.; Schubert, U. S. *Chem.—Eur. J.* **2004**, *10*, 4315.
- (28) Massey, J. A.; Temple, K.; Cao, L.; Rharbi, Y.; Raez, J.; Winnik, M. A.; Manners, I. *J. Am. Chem. Soc.* **2000**, *122*, 11577.
- (29) Fujimori, A.; Ishitsuka, M.; Nakahara, H.; Ito, E.; Hara, M.; Kanai, K.; Ouchi, Y.; Seki, K. *J. Phys. Chem. B* **2004**, *108*, 13153.
- (30) George, M.; Weiss, R. G. *Chem. Mater.* **2003**, *15*, 2879.
- (31) Peng, H. S.; Chen, D. Y.; Jiang, M. *J. Phys. Chem. B* **2003**, *107*, 12461.
- (32) Zhang, Q.; Remsen, E. E.; Wooley, K. L. *J. Am. Chem. Soc.* **2000**, *122*, 3642.
- (33) Ruokolainen, J.; ten Brinke, G.; Ikkala, O.; Torkkeli, M.; Serimaa, R. *Macromolecules* **1996**, *29*, 3409.
- (34) There was only one example of a polymer/polydiacetylene blend reported with the reversibility in both thermochromism (in a relatively narrow temperature range of 20–60 °C) and mechano-chromism. The sample was prepared by dispersing nanotubes of a chemically modified polydiacetylene polyurethane.⁶ Therefore, the polydiacetylene was reversible even before blending with polyurethane.

MA800023F